JOURNAL OF MATERIALS SCIENCE 26 (1991) 792 – 798

The influence of microstructure on fatigue crack propagation in polyoxymethylene

J. RUNT, K. P. GALLAGHER
Polymer Science Program, Department of Materials Science and Engineering, The Pennsylvania State University, Pennsylvania 16802, USA

An analysis of the influence of crystalline microstructure on fatigue crack propagation in polyoxymethylene is presented. A series of test specimens containing a variety of diverse microstructures was prepared through controlled thermal treatments of plaques from four different lots of polyoxymethylene. Extensive characterization of the crystalline microstructure was carried out in order to permit a direct comparison between the fatigue behaviour and crystalline microstructure. The degree of crystallinity and tie molecule density were both found to have a significant affect on fatigue crack propagation rate while average spherulite size did not appear to influence fatigue behaviour. Additionally, the fatigue fracture surfaces of many of the test specimens were examined. Three distinct surface topographies were observed and found to correlate with different stages of crack growth. In the region near the end of fatigue crack propagation, closely spaced surface markings that resemble fatigue striations were observed.

1. Introduction

Over the past few years we have been concerned with elucidating the role of microstructure on the dynamic fatigue behaviour of crystalline polymers. The focus of this research follows from what we believe is the most critical need at the present time; fundamental measurements on well characterized samples. We have uncovered the competitive affects of degree of crystallinity and tie molecule density in a branched polyethylene [1] as well as the importance of tie molecule density in high density polyethylene [2] and a selectively degraded polyester [3]. In the present paper we report on an extension of this research to a particularly fatigue resistant polymer, polyoxymethylene (POM).

2. Experimental details

The polymers employed in this investigation were a nucleated Celcon M90, an unnucleated Celcon M25 and two different lots of unnucleated Celcon M90 that were generously provided in the form of injection moulded plaques by Hoechst Celanese. In order to differentiate between these materials a simple identification system will be used: the two lots of unnucleated Celcon M90 are designated M90–1 and M90–2 respectively, the nucleated Celcon M90 is designated as M90-3 and the unnucleated Celcon M25 as M25. Celcon is a POM-based copolymer and will simply be referred to as polyoxymethylene. Molecular weight determination using GPC–differential viscometry show the weight average molecular weight for the M25 and M90 (all lots) to be 185 000 and 131 000 $g\,mol^{-1}$, respectively, with both having a polydispersity of 1.6.

2.1. Thermal treatments

Creating specimens with different microstructures is essential to this investigation. The microstructure of the samples can be selectively altered by carefully controlling thermal history; it was found that annealing and isothermal crystallization from different melt temperatures were most successful in creating useful samples for fatigue testing.

Many of the as-received injection-moulded plaques were first melted at 180 °C for 30 min and then quenched into ice water in order to remove any history of the injection moulding process. After this quenching, some of the samples were annealed at constant temperatures between 100 and 160 °C for 24 h. Some as-received injection-moulded samples were directly annealed without first removing the injection-moulding history. Still others were isothermally crystallized at 152 °C for 21 h after being melted at temperatures ranging from 171 to 200 °C for 30 min. A simple code to identify the thermal history of each sample has been developed: Q indicates that a sample has been quenched; QA refers to a sample that has been quenched and subsequently annealed at the temperature that directly follows the letters; AR is the designation for an as-received injection-moulded plaque with no additional thermal history; the designation ARA refers to direct annealing of an AR specimen and the digits which follow indicate annealing temperature; and ISO designates the isothermally crystallized samples with the melt temperature following.

2.2. Microstructural characterization

Heats of fusion and melting points were determined

0022–2461/91 $03.00 + .12 © *1991 Chapman and Hall Ltd.*

using a 7 series Perkin-Elmer differential scanning calorimeter (DSC). In order to obtain maximum accuracy from the experiment, samples scanned to determine heats of fusion were large, 15 to 18 mg (in order to lessen baseline effects) and samples scanned to determine melting points weighed only 0.3 to 0.5 mg (to minimize the influence of low polymer thermal conductivity). At least two samples from each specimen type were tested. Percent crystallinity was directly calculated from the measured heats of fusion, using 58 cal g^{-1} as the heat of fusion of the 100% crystalline phase [4]. Baselines defining the endothermal area were drawn from 100 to 200 °C. Lamellar thickness was not measured directly but was estimated from the melting point using the Gibbs–Thomson equation [5], using 88 ergs cm^{-2} for the end surface free energy and 180 °C as the equilibrium melting point [4].

Optical microscopy was used to determine average spherulite size. Sections, 3 μm thick, were cut from the bulk polymer at room temperature using a Reichert–Jung ultracut E microtome equipped with a glass knife. The sections were coated with silicon oil of refractive index 1.56, inserted on a glass slide with cover slip and viewed under crossed polarizers in an Olympus BHSP-300 optical microscope equipped with a PM-10AD photomicrographic system. Average spherulite size was obtained directly from recognizable spherulites in the photomicrographs.

Tie molecule density was not measured directly but evaluated from brittle tensile strength measurements as suggested by Brown and Ward [6]. Although the numerical values of the calculated tie chain densities are somewhat arbitrary, this technique provides a means to qualitatively compare and rank the various samples. The model suggested by Brown and Ward proposes that the low temperature brittle fracture stress (σ_f) is equal to the sum of the strengths of the tie molecules and the van der Waals' bonds in the interlamellar area, therefore, f_T (defined as the fraction of the interlamellar area covered by tie molecules) can be estimated from the brittle fracture stress as follows:

$$f_T = (C\sigma_f - \beta E_{iso})/\beta(E_T - E_{iso}) \quad (1)$$

where E_T is the Young's modulus of the tie molecules, E_{iso} Young's modulus for the van der Waals' bonds, β a constant of proportionality and C a stress concentration term. If identical brittle fracture tests are conducted on different samples of the same polymer, the values of C, β, E_{iso} and E_T should be constant. The following values (expected to be reasonable for POM) were used in our calculation: 120 GPa for E_T [7], 8 GPa for the E_{iso} (typical value for a glassy polymer), 0.1 for β[8]. C was chosen as 15 solely to avoid negative values of a f_T.

Measurements of brittle fracture strength were made in tension on an Instron servohydraulic testing machine, model 1331, at approximately − 120 °C and a rate of 10 cm min^{-1}. Dogbone-shaped specimens were machined from plaques possessing the same thermal histories as the samples used in the fatigue crack propagation experiments. The dogbone samples had the dimensions recommended in ASTM standard D638-72 type IV with the exception that the specimen thickness was 0.25″ (1 inch = 2.54 cm). The brittle fracture values reported in this publication are an average of values from at least five specimens.

2.3. Fatigue crack propagation

Fatigue crack propagation (FCP) rates were measured on compact-tension shaped specimens with dimensions of 2.45 × 2.3 × 0.25″. Notches were cut into each sample with a hacksaw to a length of 1.5″. The notch tip was sharpened by cutting an additional 0.1″ with a jewellers saw and further sharpened with a scalpel. An Instron servohydraulic testing machine, model 1331 with a 2500 lb (1lb = 0.453 kg) load cell, was used for all the fatigue experiments. The testing unit was operated in conjunction with a Hewlett–Packard microcomputer using a modified version of Instron's fatigue crack propagation software. Samples were tested in tension-tension using a sinusoidal waveform operating at 20 Hz and having a minimum to maximum load ratio of 0.25. Fatigue crack propagation was recorded on videotape using a GE video camera and a Magnovax video cassette recorder. Data was collected by viewing the video on a monitor that created a magnification of approximately 9 × . The fatigue crack propagation data collected from the POM specimens was analysed by plotting values of crack growth rate (da/dn) against the stress intensity factor range (ΔK) defined in ASTM E399-83.

In order to gain some insight into the deformation processes involved during crack propagation, the fracture surfaces of the fatigued samples were examined by scanning electron microscopy. An ISI-SX-40 Scanning Electron Microscope was employed using an accelerating voltage of 10 keV for all samples. All fracture surfaces were coated with a thin layer of gold to avoid sample charging.

3. Results and discussion

When fatigue data are collected over a wide range of ΔK, the log da/dn against log ΔK curve is often found to have a sigmoidal shape in which three distinct regions of crack growth rate can be identified [9]. Due to the method of data collection used in this study, it was possible in most cases to collect data over 3 to 4 decades of crack propagation rates and, for some samples, data could be obtained in all three regions of crack growth. A representative log plot of da/dn against ΔK for a POM specimen is illustrated in Fig. 1. Region I of Fig. 1 represents crack initiation. Region II represents stable crack propagation: it is in this region where the power law, $da/dn = A\Delta K^m$ [9] prevails (A and m are material variables which are a function of frequency, temperature, etc.). Finally, region III corresponds to final fracture associated with crack instability (i.e. crack growth acceleration). When making inferences about the relative fatigue resistance of the different POM samples, the available data from each test was examined completely. The growth rate data presented in this publication will, however, be limited to the stable crack growth region since this

TABLE I Microstructural characterization

Lot	Thermal history	Crystallinity (%)	T_m (°C)	L (nm)	Spherulite diameter (μm)	Brittle fracture (psi)	f_T (%)
M90-1							
	Q	66	163.1	12.8	173 ± 33	24200 ± 1500	15.3 ± 1.4
	QA140	68	165.7	15.1	142 ± 25	–	–
	QA150	68	165.6	15.0	162 ± 41	–	–
	QA160	71	168.5	18.8	142 ± 34	–	–
	ISG171	73	169.1	19.9	58 ± 17	–	–
	ISO180	73	168.6	19.0	129 ± 30	–	–
	ISO190	73	168.6	19.0	127 ± 37	19200 ± 1100	10.6 ± 1.1
	ISO198	72	168.7	19.2	141 ± 40	–	–
	AR	67	162.7	12.5	96 ± 25	–	–
	ARA130	70	162.9	12.7	116 ± 27	26600 ± 1000	17.4 ± 0.9
	ARA160	71	165.5	14.9	102 ± 20	24200 ± 3100	15.2 ± 2.9
M90-2							
	Q	64	161.6	11.8	52 ± 13	22200 ± 1300	13.4 ± 1.2
	QA100	68	162.8	12.6	49 ± 20	19000 ± 1200	10.4 ± 1.1
	QA130	66	163.6	13.2	38 ± 16	20400 ± 2000	11.7 ± 1.9
	QA150	68	166.1	15.6	36 ± 14	–	–
	QA160	68	167.1	16.8	65 ± 16	20400 ± 2100	11.7 ± 1.9
	ISO171	72	170.0	21.7	39 ± 7	15100 ± 3300	6.8 ± 3.1
	ISO180	72	168.9	19.5	73 ± 18	15000 ± 2200	6.7 ± 2.0
	ISO200	71	169.5	20.6	83 ± 20	10900 ± 2000	1.9 ± 1.9
M90-3							
	Q	66	163.0	12.7	18 ± 4	22600 ± 900	13.7 ± 0.8
	ISO180	74	170.8	23.5	–	–	–
	ISO190	–	–	–	19 ± 5	–	–
	ISO200	72	170.4	22.6	19 ± 4	–	–
M25							
	Q	63	161.1	11.5	34 ± 8	22300 ± 1300	13.4 ± 1.2

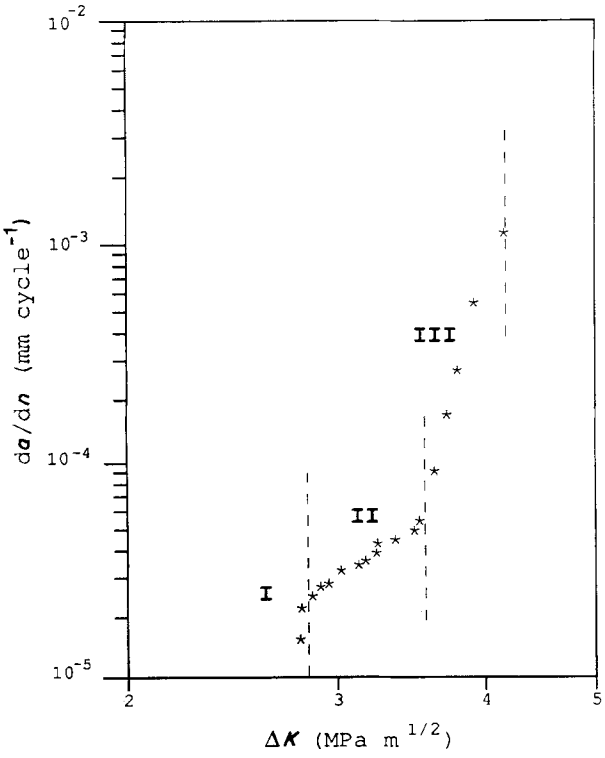

Figure 1 Typical example (ARA160) of a POM fatigue crack growth rate plot illustrating the sigmoidal shape of the curve and the three regions of fatigue crack growth response.

data was found to be the most reproducible. Additionally, multiple samples of each type were tested so that the potential experimental error could be realized. Due to the fact that only relatively small microstructural differences exist between the samples, only correspondingly small or subtle changes were expected in the FCP data, therefore, knowing the scatter that can exist in the da/dn–ΔK plots, it is less likely that any erroneous conclusions would be drawn. Additionally, semi-log plots are often utilized when displaying the data in order for shifts in the da/dn–ΔK curve to be more easily distinguished.

As mentioned previously, in order to be able to directly relate the observed fatigue results to the microstructure, the microstructure of each sample must be carefully characterized. The results of this extensive characterization can be seen in Table I.

3.1. Annealing

M90-2 quenched samples annealed between 100 and 160 °C were found to exhibit a slight increase in crystallinity (about 4%) and lamellar thickness upon annealing and perhaps a reduction in tie molecule density although the change is not outside of the quoted errors (see Table I). FCP results illustrated in Fig. 2 reveal a general increase in fatigue resistance

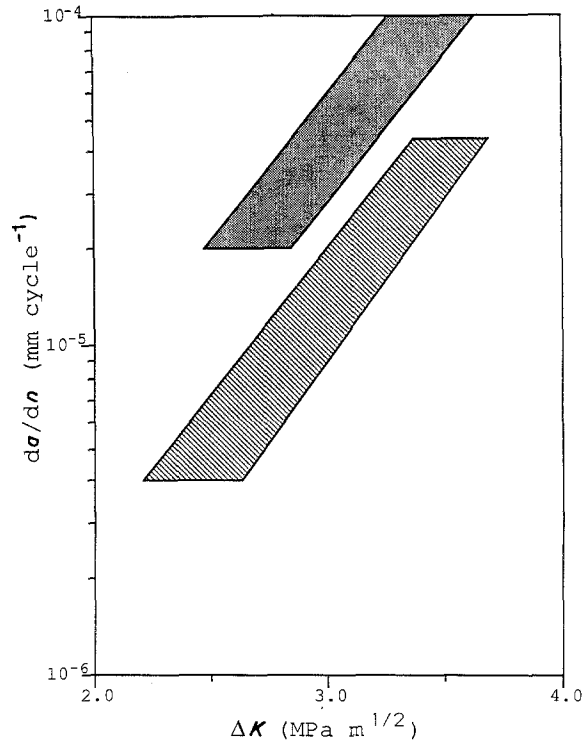

Figure 2 Comparison of the region II FCP rates between quenched (■) and quenched-annealed (▨) samples.

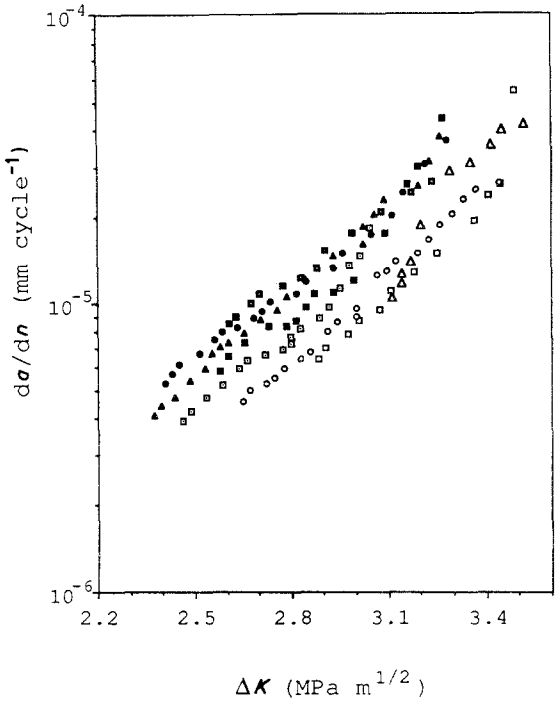

Figure 3 FCP rates of M90-2 samples annealed at temperatures between 100 °C and 160 °C (region II crack growth only). (▲QA100, ●QA100, ■QA130, ■QA130, ⊡QA150, □QA150, △QA160, ○QA160)

upon annealing. The bands employed in Fig. 2 and subsequent figures represent the entire variability of the data and not just one standard deviation. The same trend, increasing fatigue resistance upon annealing, was also found among the QA-M90-1 samples. The small increase in crystallinity seems to play a significant role in enhancing the fatigue resistance, since the possible reduction in tie molecule density would be expected to produce the opposite effect. This result is in agreement with the findings of others [1, 10] and is consistent with the idea that in a more crystalline specimen a greater amount of energy would be required to deform a unit volume of material.

Generally, lamellar thickness (L) is not considered as important as degree of crystallinity, supermolecular structure or tie molecule density in dictating mechanical properties. However, several publications [11–14] have proposed the importance of L on yield strength and modulus. For example, one of the earliest ideas was one in which spherulitic crystalline polymers were treated as fibre-reinforced composites. This theory assumes that the lamellae are rigid rod-like structures in an amorphous, rubbery matrix. The key parameter in this composite theory is the aspect ratio which is defined as the ratio of twice the length to the thickness of the reinforcing fibre. For spherulitic polymers, the arms of the spherulite are considered the fibres, and the aspect ratio then becomes the spherulite diameter lamellar thickness. For the POM specimens under investigation here, the aspect ratios are, however, estimated to be in excess of 1000 and outside the range expected to influence mechanical properties.

A small shift in the stable da/dn–ΔK region appears to exist between samples annealed at 100 and 130 °C and those annealed at higher temperatures indicating that annealing at a higher temperature increases fatigue resistance (see Fig. 3). In this set of samples, however, the only distinguishable difference in any of the microstructural parameters is in lamellar thickness. A similar trend was observed in samples annealed directly from the as-received M90-1 lot, where the ARA160 samples were found to be slightly more fatigue resistant than the ARA 130 samples. Again, a small increase in lamellar thickness was the only detectable change in the microstructural parameters (expected experimental error in L roughly $\pm$ 1 nm). In light of this observation, the possible influence of lamellar thickness on fatigue behaviour cannot be ruled out. Since the degree of crystallinity, however, appears to be a dominating factor and is expected to increase with annealing temperature, it is possible that these relatively small reductions in FCP rate are due to increases in degree of crystallinity that are too small to be detected by DSC.

3.2. Isothermal crystallization

Among the isothermally crystallized samples the average spherulite diameter was found to change from about 58 to 141 μm (i.e. M90-1, ISO171 through ISO198) while percent crystallinity and lamellar thickness were found to remain constant. Based on the available brittle fracture test results (from M90-2), tie molecule density was also not expected to change significantly with the possible exception of ISO198. Therefore, any change in FCP rate was expected to be directly related to average spherulite size. It can be seen in Fig. 4 that no significant change in fatigue resistance was detected, and therefore, average spherulite size (at least in the size range under investigation) has no apparent affect on FCP behaviour. This result

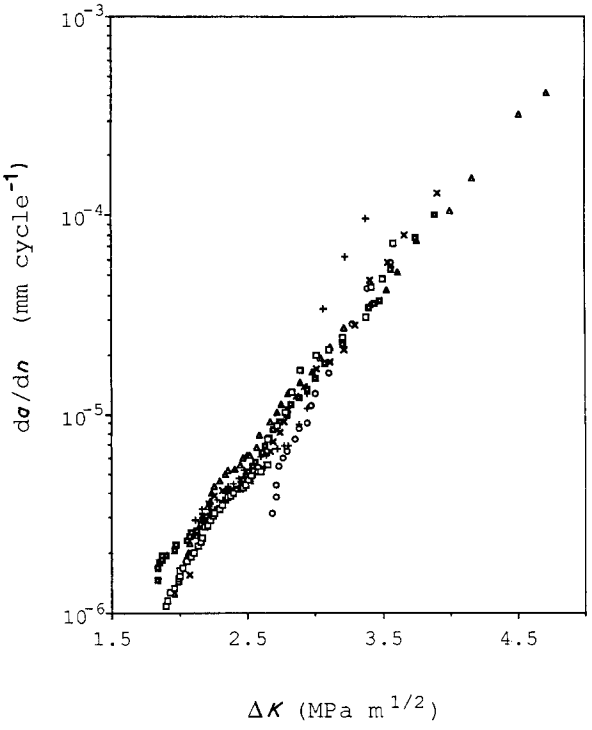

Figure 4 FCP rate comparison among samples isothermally crystallized at 152 °C from different melt temperatures. (○ISO171, ▲ISO171, + ISO180, × ISO180, ■ISO190, □ISO198).

is contrary to the findings of Friedrich [15] and Andrews and Walker [16]. The propagating flaw is, however, proceeded by a significant zone of plastic deformation and is not expected to directly encounter the spherulites. It seems, therefore, reasonable that the fatigue behaviour would be unaffected by average spherulite size, or for that matter, spherulite size distribution.

Surprisingly, the isothermally crystallized samples appear to have about the same fatigue resistance as the quenched samples. With the 6 to 7% increase in crystallinity and 6 to 10 nm increase in lamellar thickness over the quenched materials, it may be anticipated, based on the above observations, that the isothermally crystallized samples would be more fatigue resistant. There is also, however, a rather significant reduction in tie molecule density in the isothermal samples compared to those that have been quenched. Previously, FCP rates have been found to increase with decreasing tie molecule density [1–3] and therefore, it seems likely that the affect of degree of crystallinity (and perhaps L) has been more or less balanced by the reduction in tie molecule density. A reduction in fatigue resistance with decreasing tie molecule density appears to be reasonable since tie molecules interconnect crystalline regions and, therefore, by their nature tend to resist deformation. Additionally, tie molecules are also expected to play a significant role in promoting crazing which is the predominant mechanism through which the material can dissipate energy to further resist deformation.

3.3. Nucleation

Nucleating the M90 Celcon resulted in a morphology in which the average spherulite diameter was only about 19 μm. This leads nicely to another probe into the influence of spherulite size on FCP. Quenched and isothermally crystallized M90-3 POM samples were prepared with the same thermal histories as the unnucleated Celcon M90. Samples were obtained with average spherulite diameters ranging from 19 μm in the nucleated samples to over 100 μm in the unnucleated ones while all the other measured microstructural parameters remained relatively constant. Additionally, the average molecular weight and distribution of all of the Celcon M90 polymers were the same within experimental error. No discernable differences were found between the FCP behaviour of the nucleated and unnucleated samples, again indicating that average spherulite size does not significantly influence fatigue resistance.

3.4. Molecular weight

Quenched samples from all four polymer lots were tested, and comparisons were made based on molecular weight (M90 against M25). Among these samples, average spherulite size was the only microstructural parameter that was not found to be constant within experimental error, but as previously concluded, it is not expected to affect FCP behaviour. Still, the results of the fatigue experiments indicate that the higher molecular weight sample is slightly more fatigue resistant (see Fig. 5). This result is consistent with recent findings [2] in which an improvement in fatigue crack resistance with molecular weight has been related to enhanced tie molecule density. The same result is expected here, but using the brittle fracture stress estimate of f_T, a difference in tie molecule density between the M90 and M25 specimens could not be detected.

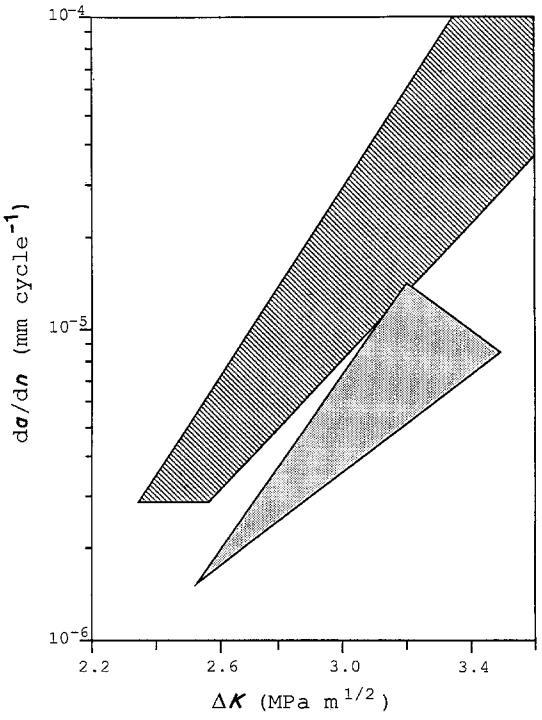

Figure 5 Comparison of the region II FCP rates of Q-M90 (▨) (all lots) and Q-M25 (□) samples.

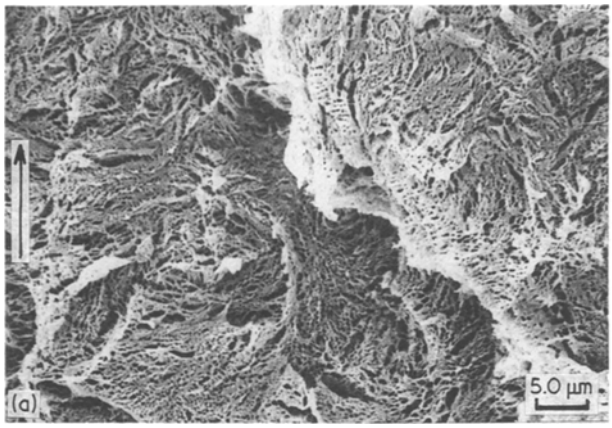

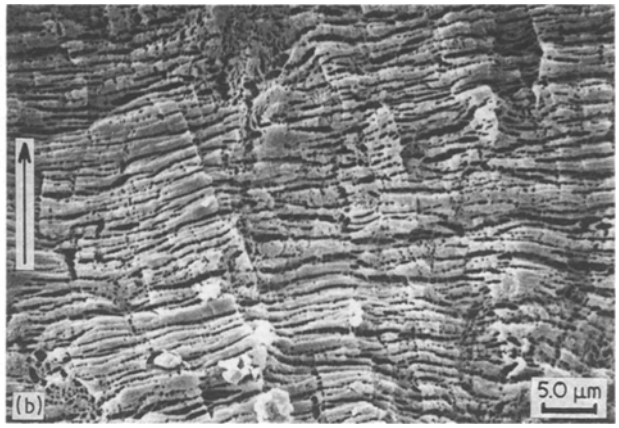

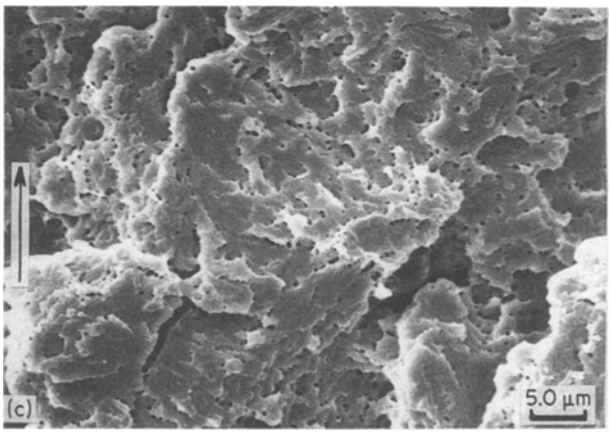

Figure 6 Typical fatigue fracture surface topography of POM (arrows indicate growth direction) (a) regions I and II of crack growth, (b) region III of crack growth, (c) region of catastrophic failure.

3.5. Fracture surfaces

In the POM specimens under investigation, three distinct regions could be identified on all of the fracture surfaces (see Fig. 6). The topography near the beginning of the crack growth (Fig. 6a) was found to be the most coarse, possessing a "drawn out" surface structure indicating the remnants of crazes. Near the end of stable crack propagation two abrupt changes in the fracture surface topography were observed that seem to indicate a change in fracture mode. One change was observed at the point of catastrophic failure and the topography from this region can be seen in Fig. 6c. The other observed change in topography occurred in a region just prior to catastrophic failure. In this region fracture surface markings that resemble fatigue striations were observed (Fig. 6b). This is the first time markings of this kind have been reported for POM. Previously, Hertzburg *et al.* [17] have reported discontinuous growth bands in POM, but nothing resembling fatigue striations. In most of the fracture surfaces explored, the markings were observed in a relatively narrow ΔK range, and the microscopic growth rate calculated from the band separation length and the macroscopically measured growth rate were generally of the same order of magnitude. In some cases, however, the markings were found to occur over several millimetres corresponding to two or three orders of magnitude increase in macroscopic growth rate while the microscopic growth rates calculated from the markings remained relatively constant. In fact, the spacings between the fatigue markings among all samples examined are indicative of growth rates only between 5×10^{-4} to 1×10^{-3} mm cycle^{-1}.

Regions containing fatigue markings were found to directly correspond with region III (illustrated in Fig. 1) of the da/dn–ΔK plots. In all of the fracture surfaces investigated, which display a discernible da/dn–ΔK curve transition from region II to region III, a corresponding change was observed on the fracture surface from a region without markings to one that contained markings. Some of the isothermally crystallized specimens were not found to contain a detectable transition to region III, and correspondingly, only a few fatigue markings immediately preceding catastrophic failure were observed.

Since fatigue tests are most often conducted at loads sufficiently below the static fracture toughness of the material, the specimens are generally in a plane strain condition. The dramatic change observed in the crack growth rate near the point of catastrophic failure could, however, conceivably result from a transition from a condition of plane strain to one of plane stress (or a mixed mode). A crude probe into the stress state of the POM compact tension specimens was made by considering the following expression that must be satisfied for the specimen to be considered to be in plane strain

$$t > 2.5\,(K_{Ic}/\sigma_y)^2 \qquad (2)$$

where t is the sample thickness, K_{Ic} the static fracture toughness and σ_y the yield strength [18]. This equation is intended for use in static fracture toughness testing, but it may provide an estimate of the stress state of a dynamic test if K_{max} and K_{min} are substituted for K_{Ic}. This approach to determining the stress condition in a fatigue test has also been suggested by Kim *et al.* [19]. For both a quenched and an isothermally crystallized sample, a value of 8000 psi was obtained as the yield stress at a rate comparable to that experienced during cyclic testing. These crude estimates of the stress condition within the samples suggest that plane strain conditions are encountered in the early stages of crack growth, but before the point of catastrophic failure a mixed mode of plane strain and plane stress may exist. Anticipating that the stress

state changes somewhere before catastrophic failure, it is possible that the transition in stress state occurs at a ΔK value associated with the slope change in the growth rate curves (see Fig. 1). Since the fatigue fracture surface markings were only produced during region III crack growth, these markings may be a result of a change in fracture mode caused by the transition to a mixed mode stress state.

Acknowledgements

The authors would like to thank the National Science Foundation (Grant DMR-8417554) and the Amoco Foundation for their support of this work. We would also like to thank Mr Cliff Boltz, Dr Andrew Auerbach and Dr Thomas Dolce of Hoechst Celanese for supplying the injection-moulded POM samples and determining molecular weights.

References

1. J. RUNT and M. JACQ, *J. Mater. Sci.* **24** (1989) 1421.
2. J. T. YEH and J. P. RUNT, *J. Polym. Sci. Polym. Phys. Ed.*, in press.
3. J. T. YEH and J. RUNT, *J. Mater. Sci.* **24** (1989) 2637.
4. J. RUNT, R. F. WAGNER and M. ZIMMER, *Macromolecules* **20** (1987) 253.
5. J. D. HOFFMAN, G. T. DAVIS and J. I. LAURITZEN, 'Treatise on Solid State Chemistry", Vol. 3, edited by N. B. Hannay (Plenum, New York, 1975).
6. N. BROWN and I. M. WARD, *J. Mater. Sci.* **38** (1983) 1405.
7. Y. TAKEUCHI, F. YAMAMOTO and K. NAKAGAWA, *J. Polym. Sci. Polym. Lett. Ed.* **22** (1984) 159.
8. A. KELLY, "Strong Solids", 2nd edn. (Clarendon, Oxford 1973) p. 10.
9. R. W. HERTZBERG and J. A. MANSON, "Fatigue of Engineering Plastics" (Academic, New York 1980).
10. A. RAMIREZ, P. M. GAULTIER, J. A. MANSON and R. W. HERTZBERG, "Fatigue in Polymers" (Plastics and Rubber Institute., London, 1983) p. 31.
11. E. H. ANDREWS, *Pure Appl. Chem.* **39** (1974) 179.
12. J. PATEL and P. J. PHILLIPS, *J. Polym. Sci., Polym. Lett. Edn.* **11** (1972) 771.
13. B. CRIST, C. J. FISHER and P. R. HOWARD, *Macromolecules* **22** (1989) 1709.
14. R. POPLI and L. MANDELKERN, *J. Polym. Sci., Polym. Phys. Edn.* **25** (1987) 441.
15. K. FRIEDRICH, Proceedings of the 9th Conference on Scanning Electron Microscopy, German Society for Testing Materials (DVM), Stuttgart, FRG, (1979) 173.
16. E. H. ANDREWS and B. J. WALKER, *Proc. R. Soc. Lond.* **A325** (1970) 57.
17. R. W. HERTZBERG, M. D. SKIBO and J. A. MANSON, *J. Mater. Sci.* **13** (1978) 1038.
18. D. BROEK, "Elementary Engineering Fracture Mechanics", 4th edn, (Martinus Nijhoff, Dordrecht, 1986).
19. H. KIM, R. W. TRUSS, Y. MAI and B. COTTERELL, *Polymer* **29** (1988) 268.

Received 22 September 1989
and accepted 26 February 1990